Optimum design of a multi-stage reverse osmosis process for the production of highly concentrated apple juice

M. A. Al-Obaidi [1, 2], C. Kara- Zaïtri [1] and I. M. Mujtaba [1, *]

[1] Chemical Engineering, School of Engineering, University of Bradford, Bradford, West Yorkshire BD7 1DP, UK

[2] Middle Technical University, Iraq – Baghdad

***Corresponding author, Tel.: +44 0 1274 233645**

E-mail address: I.M.Mujtaba@bradford.ac.uk

Abstract

Reverse Osmosis (RO) membrane process has been commonly used for clarification and concentration of apple juice processes, due to significant advance in membrane technology, requirements for low energy and cost, and effective retention of aroma components. In this paper, a multi-stage RO industrial full-scale plant based on the MSCB 2521 RE99 spiral-wound membrane module has been used to simulate the process of concentrating apple juice and to identify an optimal multi-stage RO process for a specified apple juice product of high concentration measured in Brix. The optimisation problem is formulated as a Nonlinear Programming (NLP) problem with five different RO superstructures to maximise the apple juice concentration as well as the operating parameters such as feed pressure, flow rate and temperature are optimised. A simple lumped parameter model based on the solution-diffusion model and the contribution of all sugar species (sucrose, glucose, malic acid, fructose and sorbitol) to the osmotic pressure is assumed to represent the process. The study revealed that the multi-stage series RO process can optimise the product concentration of apple juice better than other configurations. It has been concluded that the series configuration of twelve elements of 1.03 m^2 area improves the product apple juice concentration by about 142% compared to one element. Furthermore, the feed pressure and flow rate were found to have a significant impact on the concentration of the apple juice.

***Keywords*:** Apple Juice Concentration; Spiral-wound Reverse Osmosis; Multi-stage RO network; Optimisation; Nonlinear Programming.

1. Introduction

The fruit juice industry concentrates juices to remove excess water, enhance product stability and reduce transportation costs. Membrane technology is commonly used in various

separation and production methods of fruit juices and fermented beverages. Specifically, reverse osmosis (RO) can be counted as a prominent process in fruit juice concentration due to its ability to effectively retain the flavour and concentrate the juice without requiring high temperature and energy consumption (Álvarez *et al.*, 1997; Kozák *et al.*, 2008). Many experimental studies reported that the process of fruit juice evaporation has a negative impact on taste compound's retention by losing a 90% of volatile aroma compounds (Olsson and Trägårdh, 1999; Pozderovic´*et al.*, 2006). This is why the RO technology was a good condition in respect of improved production of fruit juice concentration while maintaining sensory, aroma and nutritional characteristics (Cassano *et al.*, 2007; Jesus *et al.*, 2007). Also, this process minimises the thermal damage of fruit juice due to using low temperature (4 to 50 °C) operation (Merson *et al.*, 1980; Girard and Fukumoto, 2000). Karlsson and Trägårdh (1997) counted the membrane technology as a successful separation technique that minimises the change of aroma compositions in addition to distillation, partial condensation, adsorption, and fluid extraction processes. The RO process is a well-recognized technique for concentrating aqueous solutions within a limit of 25 to 30 °Brix (due to the high osmotic pressure of concentrated apple juices). This is quite below the typical value of 45 to 60 °Brix gained by the evaporation process but it consumes higher energy (Pepper, 1990; Araujo and Maciel, 2005).

The concentration of apple juice using the RO process is mainly affected by the sequence of operating parameters of feed pressure, temperature, and flow rate as reported in many studies (Álvarez *et al.*, 1997; Sheu and Wiley, 1983: Sheu and Wiley, 1984; Álvarez *et al.*, 1998; Álvarez *et al.*, 2001). Álvarez *et al.* (1998) studied the impact of operating pressure and flow rate on the permeation of apple juice through an individual spiral-wound RO aromatic polyamide membrane type MSCB 2521 R99. The rejection of aroma compounds was observed to increase with the pressure and flow rate in the range of considered operating conditions. Also, Matsuura *et al.* (1974a) affirmed that low operating temperature of the RP process can increase the retention of aroma components. Sheu and Wiley (1983) confirmed that the processing capacity of apple juice concentration is increased due to an increase in the operating temperature between 20 to 60 °C. Chou *et al.* (1991) deduced that lowering operating temperature and maximising the operating pressure (within the permitted limits of operation) can help to provide a concentrate stream of high-flavour components content and an acceptable flux. However, Álvarez *et al.* (2001) concluded that the permeate flux and aroma rejection are increased because of increased feed flow rate in a single spiral-wound RO process. Furthermore, the inclusion of the RO process as a first step of different processes in

fruit juice concentration is considered in a commercial plant coupled with freeze concentration and/or evaporation. This technology can effectively double the operating capacity and improve both color and flavour characteristics (Girard and Fukumoto, 2000). For example, Álvarez *et al.* (2000) developed an integrated membrane process for producing apple juice and apple juice aroma concentrates, which involves clarification by microfiltration, pre-concentration by RO to 25 °Brix, and pervaporation to recover the aroma compounds and thermal evaporation to concentrate the clarified product from 25 to 72 °Brix. Matsuura *et al.* (1975) used a two stage RO process in apple juice concentration process to increase flavour components recovery. In the first stage, the concentration of fruit juice sugars is chosen, while in the second stage aroma compounds are recovered by filtering the permeate of the first stage. In this study, it is concluded that increasing pressure and lowering the processing temperature during the second stage can enhance the recovery of aroma compounds. Matsuura *et al.* (1975) have used the procedure developed by Matsuura *et al.* (1974b) to calculate the solute transport parameter for each aroma compound, then the performance of RO has been investigated utilising their earlier proposed model (Matsuura and Sourirajan, 1973).

Some combinations of different types of membranes have been suggested for juice concentration and aroma recovery. A two-stage RO configuration has been used by Walker (1990) to concentrate orange juice to 60 °Brix while retaining the fresh juice flavour. The method comprises of three elements in series of high rejection aromatic polyamide hollow fiber membranes (Stage 1) and two low-rejection membranes in series (Stage 2). The raw orange juice is fed to Stage 1, while the retentate is fed to Stage 2. Moreover, the permeates of the two stages are blended and recycled to the feed of Stage 1. This configuration has lowered the cost of orange juice production in comparison to freeze concentration processes.

Nabetani (1996) tested an integrated series of RO–NF membrane system for concentrating fruit juice. The feed juice of 10 °Brix is firstly concentrated with RO membranes to 30 °Brix and the retentate is then concentrated to 45 °Brix in NF membranes. Souza *et al.* (2013) tested the integration of the two membrane processes of RO and osmotic evaporation in order to concentrate clarified camu–camu juice with focusing on the phenolic compounds, vitamin C, and antioxidant activity of the final product. It is concluded that total solids content increased from 75 to 288 g kg^{-1} and from 288 to 566 g kg^{-1} using the RO process and osmotic evaporation respectively. This confirmed the potential of the proposed membrane integration for camu–camu juice.

A series configuration of two spiral-wound RO modules is used in the experiments of Araujo and Maciel (2005) for assessing the performance of two types of commercial polyamide membranes for concentrating orange juice. The results show that the second module improves the productivity of orange juice measured in °Brix.

An optimisation based model has been achieved by Kiss *et al.* (2004) using a series of different types of membranes including; microfiltration (MF) and RO followed by nanofiltration (NF). The sugar content in the retentate measured in °Brix and permeate flux were modelled using the linear regression of experimental data with time, and the model parameters are estimated using the Stat-graphics 5.1 program. The optimum independent variables of feed flow rate, trans-membrane pressure and temperature were investigated for optimum °Brix.

To the best of the authors' knowledge, there appears to be a gab in the use of an optimisation of the spiral-wound RO network model for apple juice concentration. There also appears that the impact of different RO network configurations for concentrating apple juice has neither been explored nor yet achieved. This paper aims to tackle this precise gap by exploring ways of maximising apple juice concentration using different RO networks configurations using an enhanced optimisation technique. This is designed to include a mathematical model of a spiral-wound RO membrane process and a set of mathematical equations for multi-stage RO network. The main objective is to identify an optimal RO configuration that can achieve high apple juice concentration measured in °Brix from a set of different networks. A small-scale plant of membrane type MSCB 2521 RE99 spiral-wound RO module (Separem, SpA, Biella, Italy) of 1.03 m^2 area (used by Álvarez *et al.*, 2002) is used in this study. Validation of the selected RO network developed is achieved by carrying out a sensitivity analysis of the operating parameters of the process (feed pressure, flow rate and temperature) on the performance of the plant.

2. Modelling of the spiral-wound Reverse Osmosis

The main objective of this section is to develop a mathematical model to predict the concentration process of apple juice using a spiral-wound membrane module and then investigate the model equations of a full-scale plant considering the interaction between several stages of the RO system.

2.1 The Assumptions

The following assumptions are made to develop the proposed process model:

1. The solution-diffusion model is used for mass transport through the module.
2. Validity of the Da Costa equation to predict the pressure drop across the membrane.
3. Validity of the film model theory to estimate the concentration polarization impact.
4. The feed osmotic pressure is only caused by all sugar species (sucrose, glucose, malic acid, fructose and sorbitol) with neglecting aroma compounds.
5. Constant atmospheric pressure on the permeate channel of 101.325 kpa.
6. The underlying process is assumed to be isothermal.

2.2. Governing Equations

Based on Assumption 1, the solution-diffusion model is valid to predict the water and solute flux of any sugar species J_w and $J_{s,i}$ (m/s, kmol/m² s) through the membrane as expressed by (Lonsdale *et al.*, 1965).

$$J_w = A_w \left[\left(\frac{\left(P_{f(in)} + P_{f(out)}\right)}{2} - P_p \right) - (\Delta\pi_{Total}) \right] \quad (1)$$

$$J_{s,i} = B_{s,i} \left(C_{m,i} - C_{p,i} \right) \quad (2)$$

Where $P_{f(in)}$, $P_{f(out)}$ and P_p (kpa) are the inlet feed pressure, outlet feed pressure and a constant permeate pressure (Assumption 5) respectively. A_w and $B_{s,i}$ (m/ kpa s, m/s) are the solvent transport coefficient and solute transport parameter of the determined sugar species for the selected aromatic polyamide membrane type (MSCB 2521 R99) respectively.

A_w was experimentally determined for the spiral-wound module using pure water and accounts for the pore distribution of the membrane, porosity, and membrane thickness. Álvarez *et al.* (2001) introduce the following correlation to show the impact of feed flow rate and operating temperature on A_w.

$$A_{w,T} = 9.059x10^{-7} \left(\frac{T}{25}\right)^{0.62} \left(\frac{36.0x10^5 \; Q_f}{400}\right)^{-0.1447} \quad (3)$$

Where Q_f and T (m³/s, °C) are the feed flow rate and operating temperature respectively. The solute transport parameter $B_{s,i}$ for all sugar compounds (sucrose, glucose, malic acid,

fructose and sorbitol) are assumed constant at 25 °C and determined in a previous work (Al-Obaidi *et al.*, 2017) as reported in Table 1. However, the transport parameter of malic acid was taken from Malalyandi *et al.* (1982).

The influence of operating temperature on solute permeability constant can be shown in Eq. (4) derived by Álvarez *et al.* (2001).

$$B_{s,i} = B_{s,i,Ref}\ exp^{0.098(T-T_{Ref.})} \quad (4)$$

Where i represents the particular sugar species under consideration. $B_{s,i}$, $B_{s,i,Ref.}$ and $T_{Ref.}$ (m^2/s, °C) are the solute parameter of any sugar compounds at operating temperature (T) and the reference temperature ($T_{Ref.}$) of 25 °C.

Souza *et al.* (2013) confirmed that the juice's osmotic pressure remained to be the main factor controlling the mass transfer. Therefore, the model developed assumed that the feed osmotic pressure is caused by the impact of all species found in sugar. However, the aroma compounds concentration is very small compared to the sugar compounds in apple juice (Álvarez *et al.*, 2001). Therefore, the total osmotic pressure $\Delta\pi_{Total}$ (kpa) will only refer to the sugar compounds without considering the impact of aroma compounds (Assumption 4). The total osmotic pressure difference of sugar can be described in Eq. (5).

$$\Delta\pi_{Total} = \left(\pi_{su,m} + \pi_{g,m} + \pi_{ma,m} + \pi_{f,m} + \pi_{so,m}\right) - \left(\pi_{su,p} + \pi_{g,p} + \pi_{ma,p} + \pi_{f,p} + \pi_{so,p}\right) \quad (5)$$

Where $\pi_{m,i}$ (kpa) is the osmotic pressure of the sugar species at the membrane wall concentration $C_{m,i}$ (kmol/m^3). While, $\pi_{p,i}$ (kpa) is the osmotic pressure at the permeate channel regarding the sugar species permeate concentration $C_{p,i}$ (kmol/m^3). Also, the symbols (su, g, ma, f and so) denote to sucrose, glucose, malic acid, fructose and sorbitol respectively. The estimation of the feed osmotic pressure caused by sucrose, glucose and malic acid is carried out using the empirical equation derived by Nabetani *et al.* (1992) as can be seen in Eq. (6).

$$\pi_{su,m} + \pi_{g,m} + \pi_{ma,m} = -\frac{R\ (T+273.15)}{V_w}\ ln\left\{\frac{\left[\frac{(1000-C_{su,m}-C_{g,m})}{M_{ww}}\right]-\left[\frac{(4\ C_{su,m})}{M_{su}}\right]-\left[\frac{(2\ C_{g,m})}{M_g}\right]}{\left[\frac{(1000-C_{su,m}-C_{g,m})}{M_{ww}}\right]-\left[\frac{(4\ C_{su,m})}{M_{su}}\right]-\left[\frac{(2\ C_{g,m})}{M_g}\right]}\right\} + \frac{R\ (T+273.15)\ C_{ma,m}}{M_{ma}} \quad (6)$$

Where R, Vw and Mww (kpa m^3/ K kmol, m^3/kmol, kg/kmol) are the gas constant, the molar volume of water and the molecular weight of water respectively. While M_{su}, M_g and M_{ma} (kg/kmol) are the molecular weights of sucrose, glucose and malic acid respectively are

reported in Table 1. Note, all the concentrations expressed in Eq. (6) are referred to the concentration of the species at the wall membrane and expressed in (kg/m³).

While, the osmotic pressure caused by fructose and sorbitol is calculated using Eqs. (7) and (8) respectively.

$$\pi_{f,m} = R\ (T + 273.15)\ C_{f,m} \quad (7)$$

$$\pi_{so,m} = R\ (T + 273.15)\ C_{so,m} \quad (8)$$

Furthermore, the osmotic pressure of any sugar species at the permeate channel is calculated using Eq. (9).

$$\pi_{i,p} = R\ (T + 273.15)\ C_{i,p} \quad (9)$$

Where *i* represents the particular sugar species under consideration.

The concentration of the sugar and aroma compounds at the wall membrane was estimated based on Assumption 3, which in turn is based on the validity of the film model theory where the solvent flux is linked to concentration polarization and mass transfer coefficient, k (m/s) by the following equation:

$$\frac{(C_{m,i} - C_{p,i})}{(C_{b,i} - C_{p,,i})} = exp\left(\frac{J_w}{k_i}\right) \quad (10)$$

$C_{b,i}$, and k_i (kmol/m³, m/s) are the bulk concentration in the feed channel and the mass transfer coefficient of any sugar species respectively. $C_{b,i}$ is taken as the average value of feed $C_{f,i}$ and retentate $C_{r,i}$ concentrations for each sugar species using Eq. (11).

$$C_{bi} = \frac{C_{f,i} + C_{r,i}}{2} \quad (11)$$

The mass transfer coefficient for any species of sugar compounds k_i (m/s) is a function of pressure, concentration, flow rate and temperature, which is calculated using the proposed equation of Schock and Miquel's (1987).

$$k_i = 0.065\ \left(\frac{D_i}{d_h}\right)\ Re_{mix}^{0.875}\ \ Sc_i^{0.25} \quad (12)$$

D_i, Re_{mix}, Sc_i and d_h (m²/s, dimensionless, m) are the diffusion coefficient of any sugar species, the Reynolds number of the mixture of five sugar compounds, the Schmidt number of any sugar species and hydraulic diameter respectively.

$$Re_{mix} = \frac{\rho_{mix}\ d_h\ \ U_b}{\mu_{mix}} \quad (13)$$

$$Sc_i = \frac{\mu_{mix}}{\rho_{mix}\ D_i} \quad (14)$$

Where ρ_{mix}, μ_{mix} and U_b (kg/m³, kg/m s, m/s) are the apple juice density and viscosity and the average bulk velocity at feed channel respectively.

The apple juice density is calculated as a function of concentration in °Brix and operating temperature (Constenla *et al.*, 1989). The inlet and outlet apple juice densities were used to calculate the apple juice density as indicated in Eqs. (15), (16) and (17).

$$\rho_{in} = \left[0.8272 + (0.3471 \exp\left(0.01\ ^\circ Brix_{in}\right)) - (5.479\ x10^{-4}\ (T + 273.15))\right] x\ 10^3 \quad (15)$$

$$\rho_{out} = \left[0.8272 + (0.3471 \exp\left(0.01\ ^\circ Brix_{out}\right)) - (5.479\ x10^{-4}\ (T + 273.15))\right] x\ 10^3 \quad (16)$$

$$\rho_{mix} = \frac{\rho_{in}+\rho_{out}}{2} \quad (17)$$

$^\circ Brix_{in}$ and $^\circ Brix_{out}$ (kg/m³) denote the inlet and outlet concentration of apple juice, which are calculated using Eqs. (18) and (19) regarding the total feed and retentate concentrations of a mixture of five sugar compounds.

$$^\circ Brix_{in} = 0.09945\left(\sum_{i=1}^{n} C_{f,i}\right) \quad (18)$$

n represents the total number of sugar compounds

$$^\circ Brix_{out} = 0.09945\left(\sum_{i=1}^{n} C_{r,i}\right) \quad (19)$$

For the above two equations, note that $C_{f,i}$ and $C_{r,i}$ are the feed and retentate concentrations of any sugar species measured in kg/m³ units.

The apple juice viscosity μ_{mix} (kg/m s) can be calculated as a function of inlet and outlet concentrations of °Brix and operating temperature using Eqs. (20), (21) and (22) (Constenla *et al.*, 1989).

$$\frac{\mu_{in}}{\mu_w} = exp\left(\frac{A\ ^\circ Brix_{in}}{100 - B\ ^\circ Brix_{in}}\right) \quad (20)$$

$$\frac{\mu_{out}}{\mu_w} = exp\left(\frac{A\ ^\circ Brix_{out}}{100 - B\ ^\circ Brix_{out}}\right) \quad (21)$$

$$\mu_{mix} = \frac{\mu_{in}+\mu_{out}}{2} \quad (22)$$

μ_w is the viscosity of water (8.94E-4 kg/m s). A and B are parameters related to the temperature and can be estimated using Eqs. (23) and (24).

$$A = -0.25801 + \frac{817.11}{(T+273.15)} \quad (23)$$

$$B = 1.8909 - 3.0212\ x10^{-3}\ (T + 273.15) \quad (24)$$

Then, the diffusion coefficient for any sugar species D_i (m²/s) can be calculated using the empirical equation proposed by Gladdon and Dole (1953) as can be seen in Eqs. (25) and (26) respectively.

$$D_i = D_s \left(\frac{\mu_w}{\mu_{mix}}\right)^{0.45} \quad (25)$$

D_s (m²/s) is referred to the diffusion coefficient of any species of sugar in a very dilute solution which is calculated using the proposed correlation of Wilke and Chang (1955).

$$D_s = \left(\frac{7.4\, x10^{-8}\, (2.6\, M_w)^{0.5}\, (T+273.15)}{(1000\, \mu_{mix})\, (1000\, V_{bp,A})^{0.6}}\right) x10^{-4} \quad (26)$$

The above equation is correlated to be compatible with the used units. M_w and $V_{bp,A}$ (kg/kmol, m³/kmol) are the molecular weight of water (18.01528 kg/kmol) and the molar volume of the sugar species at its normal boiling point. $V_{bp,A}$ values for all sugar compounds are shown in Table 1.

The process of apple juice concentration is conducted by a pressure drop along the membrane edges. Therefore, $P_{f(out)}$ is calculated using Eq. (27).

$$P_{f(out)} = P_{f(in)} - \Delta P_{drop} \quad (27)$$

Where ΔP_{drop} (kpa) is the pressure drop, which is calculated using the proposed correlation of Da Costa *et al.*, (1994).

$$\Delta P_{drop} = \left(\frac{\rho_{mix}\ U_b^2\ L\ C_{td}}{2\ dh}\right) x10^{-3} \quad (28)$$

Where C_{td} (dimensionless) is the total drag coefficient, which is calculated using Eq. (29). Also, L (m) is the membrane length. It is assumed that the spacer type (NALTEX-151-129) is used for the used spiral-wound module.

$$C_{td} = \frac{A'}{Re_{mix}^{n}} \quad (29)$$

Where A' and n (dimensionless) are the spacer characteristics given in Table 2 for the used spacer type.

$$U_b = \frac{Q_b}{W\ t_f\ \epsilon} \quad (30)$$

Q_b, W, t_f and ϵ (m³/s, m, m, dimensionless) are the bulk feed flow rate, which is calculated using Eq. (31), the membrane width, the height of the spacer channel and the void fraction of the spacer. The characteristics of the membrane and spacer are reported in Table 2.

$$Q_b = \frac{Q_f + Q_r}{2} \quad (31)$$

Q_r (m³/s) is the retentate flow rate. While, the overall solute and mass balance equations are depicted in the counter of Eqs. (32) and (33).

$$Q_f = Q_r + Q_p \quad (32)$$

$$Q_f\, C_{f,i} = Q_r\, C_{r,i} + Q_p\, C_{p,i} \quad (33)$$

Where $C_{f,i}$, $C_{r,i}$ and $C_{p,i}$ (kmol/m³) are the concentration of any sugar species in feed, retentate and permeate channel respectively. Q_p (m³/s) is the total permeate flow rate. Also, Eq. (34) is used to calculate the concentration at the permeate channel for all sugar compounds (Al-Obaidi *et al.*, 2017).

$$C_{p,i} = \frac{C_{f,i}\, B_{s,i}}{B_{s,i} + \frac{J_w}{\exp(\frac{J_w}{k_i})}} \quad (34)$$

Finally, the rejection parameter for each sugar compound (i) can be calculate using Eq. (35).

$$Rej_i = \frac{C_{f,i} - C_{p,i}}{C_{f,i}}\, x100 \quad (35)$$

The recovery of the single module is calculated using Eq. (36).

$$Rec = \frac{Q_p}{Q_f}\, x100$$

(36)

Where Q_p (m³/s) is calculated using Eq. (37).

$$Q_p = J_w\, A$$

(37)

A (m²) is the effective membrane area.

The validation of this model is carried out by implementing the model in its distributed version of one dimension against an experimental data of the apple juice concentration. The details can be found in Al-Obaidi *et al.* (2017).

2.3. Apple juice concentration plant description and mathematical modelling

The proposed RO industrial full-scale plant is consisting of four pressure vessels connected in different networks of stages. Each stage holds a maximum of two pressure vessels connected in parallel, while each pressure vessel holds a maximum of three spiral-wound RO membrane elements type MSCB 2521 R99 of (1.03 m²) area supplied by Separem Spa. (Biella, Italy) connected in series. The reason for choosing this membrane is due to the availability of water and sugar compounds transport parameters literature in comparison to other types of membranes. The five proposed superstructures schematic diagram of the RO network can be shown in Fig. 1, which is similar to the specification of an actual pilot-scale RO seawater desalination process presented by Abbas (2005).

The concentrated stream of the first stage becomes the feed stream of the second stage and so on. While, the permeate streams of three elements in a pressure vessel are coupled to form the product stream of pressure vessel. Moreover, the permeate stream of all the stages are blended to form the product stream of the plant.

The apple juice outlet concentration of the last stage is measured in °Brix, where it is considered as the objective function of the optimisation study in Section 3. The performance of a single spiral-wound membrane element has been mathematically described in Section 2.2, while the interaction between the stages and pressure vessels is presented as follows:

The complete mathematical equations that describe the overall mass and sugar species balance equations of each pressure vessel, stage and the whole plant with the inlet and outlet streams are given as follows:

$$Q_{f(plant)} = Q_{r(plant)} + Q_{p(plant)} \quad (38)$$

$$Q_{f(plant)} = Q_{f(s=1)} \quad (39)$$

$$Q_{r(plant)} = Q_{r(s=n)} \quad (40)$$

n represents the number of the used stages

$$Q_{p(Plant)} = \sum_{s=1}^{n} Q_{p(s)} \quad (41)$$

$$P_{f(in)(plant)} = P_{f(in)(s=1)} \quad (42)$$

$$P_{f(out)(plant)} = P_{f(out)(s=n)} \quad (43)$$

$$T_{(in)(plant)} = T_{(out)(plant)} \quad (44)$$

$$C_{f,i(plant)} = C_{f,i(s=1)} \quad (45)$$

i represents the particular sugar species under consideration

328 $C_{r,i(plant)} = C_{r,i(s=n)}$ (46)

329 $Q_{f(plant)}\, C_{f,i(plant)} = Q_{r(plant)}\, C_{r,i(plant)} + Q_{p(plant)}\, C_{p,i(plant)}$ (47)

330 $^{\circ}Brix_{in(plant)} = 0.09945\left(\sum_{i=1}^{n} C_{f,i(plant)}\right)$ *n* represents the number of sugar compounds

331 (48)

332 $^{\circ}Brix_{out(plant)} = 0.09945\left(\sum_{i=1}^{n} C_{r,i(plant)}\right)$ (49)

333 $Rej_{i(plant)} = \frac{C_{f,i(plant)} - C_{p,i(plant)}}{C_{f,i(plant)}}\, x100$ (50)

334 $Rec_{(plant)} = \frac{Q_{p(plant)}}{Q_{f(plant)}}\, x100$ (51)

335 $C_{f,i(s)} = C_{r,i(s-1)}$ for s ≥ 2 (52)

336 $P_{f(in)(s)} = P_{f(out)(s-1)}$ for s ≥ 2 (53)

337 $Q_{f(s)} = Q_{r(s-1)}$ for s ≥ 2 (54)

338 $Q_{r(s)} = \sum_{PV=1}^{n} Q_{r(PV)}$ *n* represents the number of the used pressure vessels per stage (55)

339 $Q_{p(s)} = \sum_{PV=1}^{n} Q_{p(PV)}$

340 (56)

341 $Q_{f(s)}\, C_{f,i(s)} = Q_{r(s)}\, C_{r,i(s)} + Q_{p(s)}\, C_{p,i(s)}$ (57)

342 $^{\circ}Brix_{in(s)} = 0.09945\left(\sum_{i=1}^{n} C_{f,i(s)}\right)$ *n* represents the number of sugar compounds

343 (58)

344 $^{\circ}Brix_{out(s)} = 0.09945\left(\sum_{i=1}^{n} C_{r,i(s)}\right)$

345 (59)

346 $Rej_{i(s)} = \frac{C_{f,i(s)} - C_{p,i(s)}}{C_{f,i(s)}}\, x100$ *i* represents any used sugar compound

347 (60)

348 $Rec_{(s)} = \frac{Q_{p(s)}}{Q_{f(s)}}\, x100$

349 (61)

350 Also, the same criterion of the model equations has been used to describe the connection

351 between the three elements inside each pressure vessel as follows.

$Q_{f(PV)(s)} = \frac{Q_{f(s)}}{n_{(PV)}}$ $n_{(PV)}$ represents the number of pressure vessels in the stage (62)

$Q_{p(PV)} = \sum_{n=1}^{e} Q_{p,e}$ e represents the number of elements per each pressure vessel (63)

$P_{f(in)(PV)} = P_{f(in)(s)}$ (64)

$P_{f(out)(PV)} = P_{f(out)(e=3)}$ $e = 3$ represents the third membrane element in PV (65)

$C_{f,i(PV)} = C_{f,i(s)}$ (66)

$C_{r,i(PV)} = C_{r,i(e=3)}$ (67)

Finally, a simulation model was developed for a spiral-wound reverse osmosis membrane module in a steady state mode and for a multi-stage plant that describe the variation of all the operating parameters along the stages using the gPROMS software (general Process Modelling System) developed by Process System Enterprise Ltd. (2001). The gPROMS Model builder provides a modelling platform for the steady state and dynamic simulation, optimisation, experiment design and parameter estimation of any process. The model equations have been solved for a given inlet plant feed flow rate, pressure, sugar compounds concentrations and temperature. Also, the proposed model can predict the variation of all parameters along the stages and the outlet apple juice product specification.

The process model presented in Section 2 can be written in the following compact form:

$f(t, x(t), \dot{x}(z), u(z), v) = 0; \quad [t_0, t_f]$

Where, t is the independent variable (time), $x(t)$ is the set of all differential and algebraic variables, $\dot{x}(t)$ represents the derivative of $x(t)$ with respect to time, $u(t)$ is the control variables and v denotes the constant parameters of the process. The time interval under consideration $[t_0, t_f]$ and function f are assumed to be continuously differentiable with respect to all their arguments.

Fig. 1. Five different tested RO networks

3. Optimisation technique

3.1 Problem description and formulation

The objective of this section is to show the development of the RO optimisation framework based on the apple juice concentration process using multi-stage RO networks as shown in Fig. 1. This involves five different RO configurations and the optimisation methodology developed enables the selection of the optimal RO network configuration that can achieve a higher concentration of apple juice measured in °Brix. The optimum design of RO network is investigated for inlet apple juice feed concentration of 10.5 °Brix with equivalent concentrations of sugar compounds as given in Table 1. These are in turn used to analyse the influence of operating parameters of the process on the juice concentration for the selected RO network. The objective function of the optimisation algorithm developed is to maximise the apple juice concentration subjected to process and module constraints. The algorithm uses the specification and geometry of a spiral-wound membrane (MSCB 2521 R99, Sparem Spa., Biella, Italy) and the module constraints of inlet pressure, flow rate and temperature as given in Table 2. It is noted that the feed of 10.5 °Brix has concentrated to a maximum value of 11.325 °Brix using the same above RO membrane at operating conditions of 34.54 atm, 5.5556E-5 m^3/s and 20 °C of feed pressure, flow rate and temperature respectively (Al-Obaidi *et al.*, 2017). This will therefore raise the product concentration by using a multi-stage RO network.

The optimisation problem is described as follows:

Given: Operating feed conditions, module specifications.

Optimise: Inlet feed pressure, flow rate and temperature (the optimisation variables).

Maximise: The product concentration of apple juice of the RO network under consideration.

Subject to: Equality (process model, Section 2) and inequality constraints (linear bounds of optimisation variables).

Therefore, the optimisation problem is represented mathematically as follows:

$$\underset{F_{b(plant)}, P_{f(plant)}, T_{(in)(plant)}}{\text{Max}} \quad {}^{\circ}Brix_{out(plant)}$$

Subject to:

Equality constraints:

Process Model: $f(z, x(z), \dot{x}(z), u(z), v) = 0; \quad [z_0, z_f]$

Inequality constraints:

$$Q_{f(plant)}{}^{L} \leq Q_{f(plant)} \leq Q_{f(plant)}{}^{U}$$

$$P_{f(in)(plant)}{}^{L} \leq P_{f(in)(plant)} \leq P_{f(in)(plant)}{}^{U}$$

$$T_{(in)(plant)}{}^{L} \leq T_{(in)(plant)} \leq T_{(in)(plant)}{}^{U}$$

Where, U and L are the upper and lower bounds of the optimisation variables. Also, the optimisation problem entails the constraints shown below of a single spiral-wound RO membrane as follows, which satisfy the maximum and minimum practical bounds of the operating conditions:

$$Q_f{}^{L} \leq Q_f \leq Q_f{}^{U}$$

$$P_{f(in)}{}^{L} \leq P_{f(in)} \leq P_{f(in)}{}^{U}$$

$$T^{L} \leq T \leq T^{U}$$

The limits of decision variables of inlet feed flow rate, pressure and temperature of a single RO membrane are given in Table 2. All these constraints are usually specified by the membrane manufacture.

Table 1. Characteristics of the sugar compounds and their inlet concentration in the model solution of 10.5 °Brix (Álvarez *et al.*, 2002, Al-Obaidi *et al.*, 2017)

Table 2. Specifications of the spiral-wound membrane element and module constraints (Álvarez *et al.*, 2002)

4. RO networks optimisation results

For the inlet feed apple juice concentration of 10.5 °Brix, the optimisation results obtained for the five scenarios of RO networks shown in Fig. 1 for two cases (one and three) of the number of elements per each pressure vessel are shown in Table 3. Also, the optimum decision variables of each RO network and its performance regarding the product concentration measured in °Brix can be shown in Table 3.

Table 3. Comparison of outlet apple juice concentration for five cases of RO networks

It is noted that scenario D has achieved the optimum product concentration of 25.44 °Brix in comparison with other scenarios with a concentration percentage increase of 142%. This is in comparison to the outputs of one element of 7.85% concentration increase. Also, it is expected that the concentration of the juice is positively proportional to the number of elements for each

pressure vessel. Interestingly, it is expected that the organic acids and flavour components are not changed after concentrating the apple juice to 25.44 °Brix. Miyawaki *et al.* (2016)

confirmed that no substantial differences were observed for the apple juice before and after concentration from 13.7 to 25.5 °Brix using a progressive freeze-concentration system. In addition, the optimisation results of Table 3 show that both operating pressure and flow rate are the most important operational parameters, which significantly affect the performance of RO membrane in respect of the optimum values of juice concentration. While, the temperature has a lower impact where the optimum °Brix can be implemented with lower than the upper temperature bound for most scenarios. Interestingly, the optimum °Brix of all the scenarios requires high operating pressure and lower feed flow rate with a range of 35 to 50 °C of temperature, which will be explained in the next section. It can be said that the optimisation methodology has selected the upper bound of operating pressure due to the necessity to overcome the high osmotic pressure of apple juice. Gostoli *et al.* (1995) confirmed that the osmotic pressure of an orange juice is increased from 15 bar to 190 bar as a result to an increase in the total solids from 11% to 60%.

The feasibility of the recent work is comparable to the performance of an integrated process of Matta *et al.* (2004) comprising ultrafiltration UF, microfiltration MF and reverse osmosis RO used for concentrating acerola juice. Specifically, the clarification and concentration of acerola juice processes were conducted in three tubular UF and MF membranes (0.05 m^2) followed by a film composite RO membrane (0.72 m^2). it was observed that juice having 7.1 °Brix is concentrated to 29.2 °Brix at operating conditions of pressure and temperature of 100 kPa, 30 °C at UF/MF membranes and 6000 kPa, 25 °C at RO membrane.

5. Analysing the impact of operating parameters on the plant product concentration

Here, the model developed is used to simulate the process, explore the sensitivity of the model to different parameters of the process, and take an overview of the outlet apple juice concentration measured in °Brix for the optimum RO network (scenario D) of four pressure vessels and twelve elements in series under the impact of varying the process parameters.

Firstly, it is important to study the impact of operating pressure, flow rate and temperature on sugar species rejection due to its relationship with the bulk and retentate concentration of apple juice.

Figs. 2, 3 and 4 illustrate the variation of sugar species rejection (sucrose, glucose, malic acid, fructose and sorbitol) as a result to increase in operating pressure at three cases of feed flow rate at constant temperature of 40 °C.

Fig. 2. Sugar species rejection as a function of operating pressure at inlet feed flow rate and temperature of 1E-3 m^3/s and 40 ℃

Fig. 3. Sugar species rejection as function of operating pressure at inlet feed flow rate and temperature of 1E-4 m^3/s and 40 ℃

Fig. 4. Sugar species rejection as a function of operating pressure at inlet feed flow rate and temperature of 3.7E-5 m^3/s and 40 ℃

The expectation that increasing inlet feed pressure will increase sugar rejection due to accelerating water flux as denoted by Eq. (1). However, it seems that this phenomenon is confirmed for medium and high feed flow rates in comparison to lower ones. This is attributed to the increase in concentration and the osmotic pressure of the feed side, which in turn increases sugar flux through the membrane and permeate concentration at lower feed flow rate conditions. Therefore, sugar retention is decreased due to an increase in operating pressure as denoted by Eq. (35). While, increasing inlet feed flow rate would increase water flux and sugar rejection, since this would reduce the concentration polarization impact as shown in Figs. 2 and 3. The same impact of inlet feed flow rate was observed by Álvarez *et al.* (2001) who concluded that the permeate flux and aroma rejection are increased due to an increase in feed flow rate of an individual single spiral-wound RO process.

The response of product concentration for the variation of both inlet feed pressure of 2200 to 4200 kpa and flow rate of 3.68E-5 to 1E-3 m^3/s at constant operating concentration and temperature of 10.5 °Brix and 40 °C respectively is shown in Fig. 5.

Fig. 5. Impact of variation in inlet feed pressure and flow rate on product concentration at fixed inlet feed concentration and temperature of 10.5 °Brix and 40 ºC

Interestingly, Fig. 5 shows that the product concentration increases markedly due to the increase in operating pressure at low feed flow rate, which is comparable to high feed flow rate conditions. It is concluded from Fig. 4 that the sugar species rejection decreases with an increase in the operating pressure at low feed flow rate in addition to an increase in water and sugar fluxes. Therefore, the retentate flow rate will be decreased and concentrated due to high

rates of filtration with higher feed residence time. Simply, increasing operating pressure can enhance the concentration of feed in the subsequent sub-sections of feed channel since the solute is retained in the wall with the diffusion of water through the membrane.

In contrast, using high feed flow rate conditions can cause a slight increase in product concentration. This event is caused by an increase of the water flux and retention parameter by increasing the operating pressure at high inlet feed flow rate conditions (Fig. 2). Simply, increasing inlet feed flow causes a reduction of osmotic pressure of feed channel and wall membrane concentration, which in turn reduces solute flux through the membrane. However, at higher operating feed flow rate, the progress of retentate concentration along the membrane channel is noticeably lower than the case of lower feed flow rate conditions, due to lower residence time of filtration. Additionally, Fig. 6 shows an inverse relation between the retentate sugar concentration and operating feed flow rate at three operating pressures and constant temperatures. Consequently, the outlet product concentration will be increased as a function of the decreasing operating feed flow rate at any operating pressure.

Fig. 6. Sugar species retention concentration verse operating pressure at two inlet feed flow rates and inlet feed concentration and temperature of 3.68E-5 and 1E-3 m^3/s, 10.5 °Brix and 40 °C

The response of product concentration for the variation of both inlet feed pressure of 2200 to 4200 kpa and inlet feed temperature of 30 to 45 °C at constant operating concentration and flow rate of 10.5 °Brix and 4E-5 m^3/s respectively is shown in Fig. 7.

Fig. 7. Impact of variation in inlet feed pressure and temperature on product concentration at fixed inlet feed concentration and flow rate of 10.5 °Brix and 4E-5 m^3/s

Fig. 7 shows that the temperature variation has inconsiderable impact on product concentration in comparison with the operating pressure. Interestingly, Figs 8 and 9 clearly show that the rejection of all sugar species decreases due to an increase in the operating temperature in two different feed flow rates, which is quite similar to the findings of aroma compounds retention in different study of Al-Obaidi *et al.* (2017). Moreover, Chou *et al.* (1991) observed that an increase in operating temperature from 20 °C to 40 °C tends to increase the permeation rate at the penalty of lowering the retention of volatiles compounds. The probable explanation for this can be that by increasing feed temperature, density and viscosity decrease and water permeation rate through membrane and diffusivity parameter increase. Also, the solubility of sugar species increases and higher diffusion rate of sugar through the membrane is possible due to the variation of pore size of the polymeric membrane, which ultimately reduces the rejection parameter and reduces the retentate flow rate with somehow elevated product concentration. Zainal et al. (2000) studied the impact of operating temperature on the physical properties of pink guava juice and showed that increasing the temperature causes a decrease in consistency coefficient, which result in an increase in the flow behaviour index due to less resistance flow.

Fig. 8. Sugar species rejection as a function to operating feed temperature at inlet feed concentration and flow rate of 10.5 Brix and 3.68E-5

Fig. 9. Sugar species rejection as a function to operating feed temperature at inlet feed concentration and flow rate of 10.5 Brix and 1E-3

6. Conclusions

The process of apple juice concentration using a multi-stage RO network based on a spiral-wound module is mathematically modelled to simulate and optimise the concentration of apple juice taking into account the limits of operation and the constraints of both the module and RO layout. Accordingly, several differential equations have been developed based on the solution-diffusion model taking into account the effect of all sugar species in the calculation of osmotic pressure. Also, the model incorporates the physical properties of apple juice using the empirical equations that shows the impact of concentration and temperature. The optimisation results have shown that the series configuration of twelve elements of 1.03 m^2 area can increase the product concentration of apple juice by about 142% in comparison to

one element. Furthermore, the impact of the main operating parameters of feed pressure, flow rate and temperature on the product specification were investigated for the optimum RO network. It is concluded that the feed pressure and flow rate have weighty impact on apple juice concentration in comparison to inconsiderable impact of feed temperature. Further work is planned to optimise the apple juice concentration by weighing the impact of the high module area and different layouts of recycled RO network.

References

Abbas A., 2005. Simulation and analysis of an industrial water desalination plant. *Chemical Engineering and Processing*, 44, 999-1004.

Al-Bastaki N. and Abbas A., 2003. Permeate recycle to improve the performance of a spiral-wound RO plant. *Desalination*, 158, 119-126.

Al-Obaidi M.A., Kara-Zaïtri C. and Mujtaba I.M., 2017. Development of a mathematical model for apple juice compounds rejection in a spiral-wound reverse osmosis process. *Journal of Food Engineering*, 192, 111-121.

Álvarez V., Álvarez S., Riera F., and Álvarez R., 1997. Permeate flux prediction in apple juice concentration by reverse osmosis. *Journal of Membrane Science*, 127, 25-34.

Álvarez S., Riera F., Álvarez R. and Coca J., 1998. Permeation of apple juice compounds in reverse osmosis. *Separation Purification Technology*, 14, 209-220.

Álvarez S., Riera F.A., Álvarez R., Coca J., Cuperus F.P., Th Bouwer S., Boswinkel G., van Gemert R.W., Veldsink J.W., Giorno L., Donato L., Todisco S., Drioli E., Olsson J., Trägårdh G., Gaeta S.N. and Panyor L., 2000. A new integrated membrane process for producing clarified apple juice and apple juice aroma concentrate. *Journal of Food Engineering*, 46, 109-125.

Álvarez S., Riera F., Álvarez R. and Coca J., 2001. Prediction of flux and aroma compounds rejection in a reverse osmosis concentration of apple juice model solutions. *Industrial Engineering Chemistry Research*, 40(22), 4925-4934.

734 Álvarez S., Riera F., Álvarez R. and Coca J., 2002. Concentration of apple juice by reverse
735 osmosis at laboratory and pilot-plant scales. *Industrial Engineering Chemistry Research*, 41,
736 6156-6164.

737 Araujo W. A. and Maciel M. R. W., 2005. Reverse osmosis concentration of orange juice
738 using spiral wound membranes. *Alimentos e Nutrição Araraquara*, 16(3), 213-219.

739 Cassano A., Donato, L. and Drioli, E., 2007. Ultrafiltration of kiwifruit juice: Operating
740 parameters, juice quality and membrane fouling. *Journal of Food Engineering*, 79, 613-621.

741 Chou F., Wiley R. C., and Schlimme D. V., 1991. Reverse osmosis and flavor retention in
742 apple juice concentration. *Journal of Food Science*, 56(2), 484-487.

743 Constenla D. T., Lozano J. E. and Crapiste G. H., 1989. Thermo-physical properties of
744 clarified apple juice as a function of concentration and temperature. *Journal of Food Science*,
745 54(3), 663-668.

746 Da Costa A.R., Fane A.G. and Wiley D.E., 1994. Spacer characterization and pressure drop
747 modelling in spacer-filled channels for ultrafiltration. *Journal of Membrane Science*, 87, 79-
748 98.

749 Geraldes V., Pereira N. E. and de Pinho M. N., 2005. Simulation and Optimisation of
750 Medium-Sized Seawater Reverse Osmosis Processes with Spiral-Wound Modules. *Industrial*
751 *and Engineering Chemistry Research*, 44, 1897-1905.

752 Girard B. and Fukumoto L. R., 2000. Membrane processing of fruit juices and beverages: A
753 review. *Critical Reviews in Food Science and Nutrition*, 40(2), 91-157.

754 Gladdon J. K. and Dole M., 1953. Diffusivity determination of sucrose and glucose solutions.
755 *J. Am. Chem. Soc*., 75, 3900-3904.

756 Gostoli C., Bandini S., Di Francesca R., and Zardi G., 1995. Concentrating fruit juices by
757 reverse osmosis—the low retention—high retention method. *Fruit Process*, 6, 183-193.Gurak
758 P. D., Cabral L. M. C., Rocha-Leão M H. M. and Matta V. M., 2010. Quality evaluation of
759 grape juice concentrated by reverse osmosis. *Journal of Food Engineering*, 96, 421-426.

760 Hatfield G. B. and Graves G. W., 1970. Optimisation of a reverse osmosis system using
761 nonlinear programming. *Desalination*, 7, 147-177.

762 Jesus D. F., Leite M. F., Silva L. F. M., Modesta R. D., Matta V. M. and Cabral L. M. C.,
763 2007. Orange (*Citrus sinensis*) juice concentration by reverse osmosis. Journal of Food
764 Engineering, 81, 287-291.

765 Kiss I., Gy V. and Bekassy-Molnar E., 2004. Must concentrate using membrane technology.
766 *Desalination*, 162, 295-300.

767 Karlsson H. O. E. and Trägårdh G., 1997. Aroma Recovery During Beverage Processing.
768 *Journal of Food Engineering*, 34, 159-178.

769 Khayet M., Cojocaru C. and Essalhi M., 2011. Artificial neural network modeling and
770 response surface methodology of desalination by reverse osmosis. *Journal of Membrane*
771 *Science*, 368, 202-214.

772 Kozák A., Bánvölgyi S., Vincze I., Kiss I., Békássy-Molnár E., and Vatai G., 2008.
773 Comparison of integrated large scale and laboratory scale membrane processes for the
774 production of black currant juice concentrate. *Chemical Engineering and Processing:*
775 *Process Intensification*, 47(7), 1171-1177.

776 Lonsdale H. K., Merten U. and Riley R. L., 1965. Transport properties of cellulose acetate
777 osmotic membranes. *Journal of Applied Polymer Science*, 9, 1341-1362.

778 Malalyandi P., Matsuura T. and Sourirajan S., 1982. Predictability of membrane performance
779 for mixed solute reverse osmosis systems. System cellulose acetate membrane-D-Glucose-
780 D,L-Malic acid-water. *Industrial and Engineering Chemistry Process Design and*
781 *Development*, 21, 277-282.

782 Matsuura T., and Sourirajan S., 1973. Physicochemical criteria for reverse osmosis separation
783 of monohydric and polyhydric alcohols in aqueous solutions using porous cellulose acetate
784 membranes. *Journal of Applied Polymer Science*, 17(4), 1043-1071.

785 Matsuura T., Baxter A. G., and Sourirajan S., 1974a. Studies on reverse osmosis for
786 concentration of fruit juice. Journal of Food Science, 39(4), 704-711.

787 Matsuura T., Bednas M. E., Dickson J. M., Sourirajan S., 1974b. Polar and steric effects in
788 reverse osmosis. *Journal of Applied Polymer Science*, 18, 2829-2846.

789 Matsuura T., Baxter A. G., and Sourirajan S., 1975. Reverse osmosis recovery of flavor
790 components from apple juice waters. *Journal of Food Science*, 40(5), 1039-1046.

791 Matta V. M., Moretti R. H., and Cabral L. M. C., 2004. Microfiltration and reverse osmosis
792 for clarification and concentration of acerola juice. *Journal of Food Engineering*, 61, 477-
793 482.

794 Merson R. L., Paredes G., and Hosaka D. B., 1980. Concentrating fruit juices by reverse
795 osmosis. In Ultrafiltration membranes and applications (p. 405). New York: Plenum Press.

796 Miyawaki O., Gunathilake M., Omote C., Koyanagi T., Sasaki T., Take H., Matsuda A.,
797 Ishisaki K., Miwa S., and Kitano S., 2016. Progressive freeze-concentration of apple juice
798 and its application to produce a new type apple wine. *Journal of Food Engineering*, 171, 153-
799 158.

800 Nabetani H., Nakajima M., Watanabe A., Nakao S. and Kimura S., 1992. Prediction of the
801 flux for the reverse osmosis of a solution containing sucrose and glucose. *Journal of*
802 *Chemical Engineering of Japan*, 25(5), 575-580.

803 Nabetani H., 1996. Development of a membrane system for highly concentrated fruit juice.
804 *Journal of Membrane* (Japanese), 21(2), 102-108.

805 Olsson J. and Gun Trägårdh, 1999. Influence of feed flow velocity on pervaporative aroma
806 recovery from a model solution of apple juice aroma compounds. *Journal of Food*
807 *Engineering*, 39, 107-115.

808 Pepper D., 1990. RO for improved products in the food and chemical industries and water
809 treatment. *Desalination*, 77, 55-71.

810 Pozderovic´ A., Moslavac T. and Pichler A., 2006. Concentration of aqueous solutions of
811 organic components by reverse osmosis I: Influence of trans-membrane pressure and
812 membrane type on concentration of different ester and aldehyde solutions by reverse osmosis.
813 Journal of Food Engineering, 76, 387-395.

814 Process System Enterprise Ltd., gPROMS Introductory User Guide. London: Process System
815 Enterprise Ltd., (2001).

816 Sassi K. M. and Mujtaba I. M., 2012. Effective design of reverse osmosis based desalination
817 process considering wide range of salinity and seawater temperature. *Desalination*, 306, 8-16.

818 Schock G. and Miquel A., 1987. Mass transfer and pressure loss in spiral wound modules.
819 *Desalination*, 64, 339-352.

820 Sheu M. J. and Wiley R. C., 1983. Preconcentration of apple juice by reverse osmosis.
821 *Journal of Food Science*, 48(2), 422-429.

822 Sheu M. J. and Wiley R. C., 1984. Influence of reverse osmosis on sugar retention in apple
823 juice concentration. *Journal of Food Science*, 49(1), 304-305.

824 Souza A. L. R., Monica Pagani M., Dornier M., Gomes F. S., Renata Tonon V., Cabral L. M.
825 C., 2013. Concentration of camu–camu juice by the coupling of reverse osmosis and osmotic
826 evaporation processes. *Journal of Food Engineering*, 119, 7-12.

827 Walker J. B., 1990. Reverse osmosis concentration of juice products with improved flavor.
828 US Patent 4,959,237.

829 Wilke C. R. and Chang P., 1955. Correlation of diffusion coefficients in dilute solutions.
830 *A.I.Ch.E. Journal*, 1(2), 264-270.

831 Zainal B. S., Abdul Rahman R., Ariff A. B., Saari B. N., Asbi B. A., 2000. Effects of
832 temperature on the physical properties of pink guava juice at two different concentrations.
833 *Journal of Food Engineering*, 43, 55-59.

834

835

836

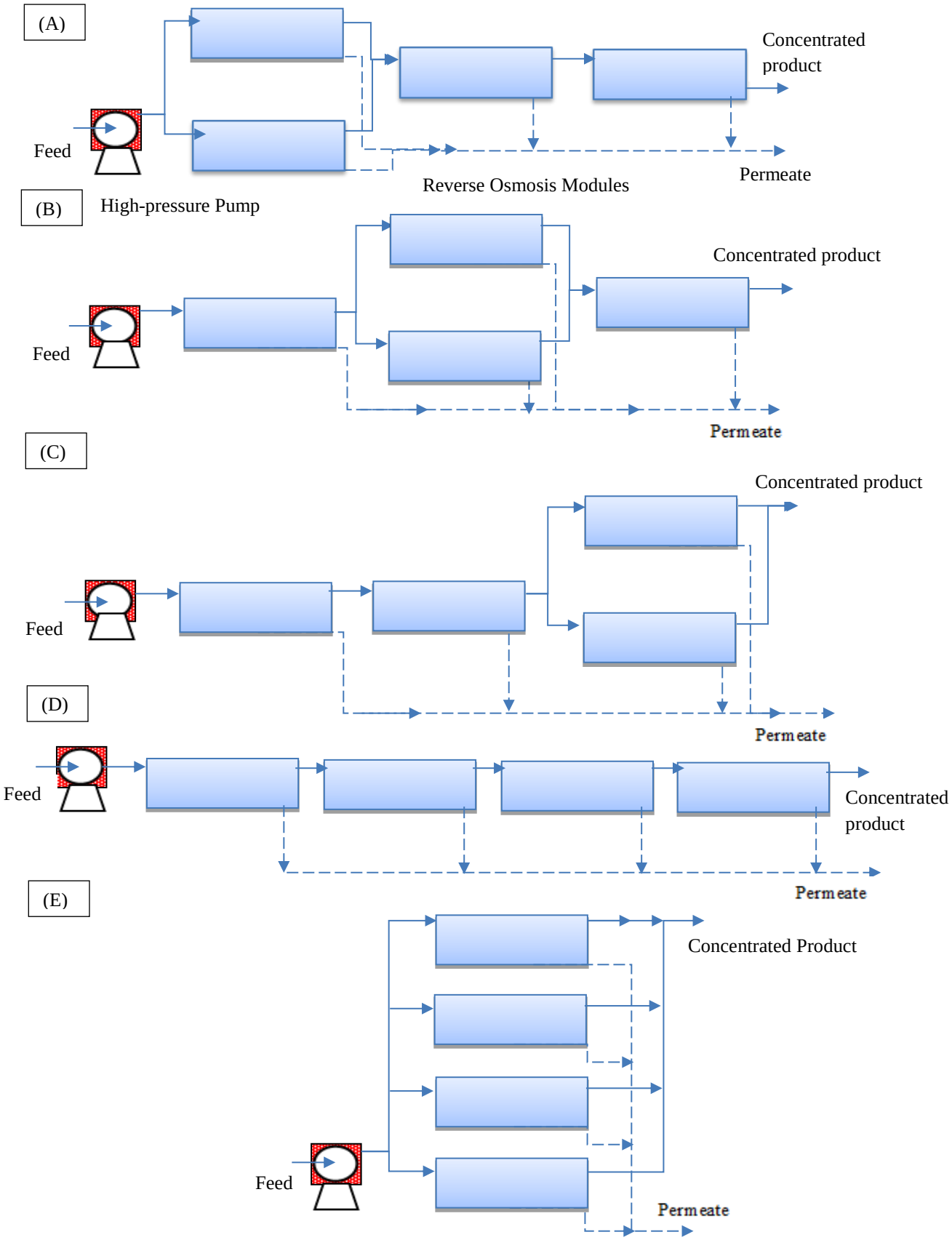

837

838 **Fig. 1**. Five different tested RO networks

Table 1. Characteristics of the sugar compounds and their inlet concentration in the model solution of 10.5 °Brix (Álvarez *et al.*, 2002, Al-Obaidi *et al.*, 2017)

Compound	Molecular weight M_{wt}, (kg/kmol)	Concentration $C_{b(0)}$, (kmol/m³)	Molar volume, $V_{bp,A}$ (m³/kmol)	Sugar compound transport parameter, $B_{s,25\,°C}$ (m/s)
sucrose	342	0.0355	0.2156	2.3299E-10
glucose	180	0.1380	0.1169	6.1146E-8
malic acid	134	0.0291	0.0833	5.4000E-8
fructose	180	0.3407	0.1063	4.2660E-8
sorbitol	182	0.0184	0.1223	5.3158E-8

Table 2. Specifications of the spiral-wound membrane element and module constraints (Álvarez *et al.*, 2002)

Make	**Sparem Spa. (Biella, Italy)**
Membrane type and configuration	MSCB 2521 R99, Spiral-wound, Polyamide membrane
Active surface area (A) (m^2)	1.03
Feed and permeate spacer thickness (t_f) (m)	7E-4
Membrane sheet length (L) and width (W) (m)	0.44 and 2.3409
Hydraulic diameter (m)	9.6E-4
Max. operating pressure (kpa)	4200
Max. operating temperature (°C)	50
Min. and Max. feed flow rate (m³/s)	2.5E-5 – 1.6667E-4
Spacer type	NALTEX-151-129
A' (dimensionless) *	7.38
n (dimensionless) *	0.34
ϵ (dimensionless) **	0.9058

*: Da Costa *et al.* (1994)
**: Al-Bastaki and Abbas (2003)

Table 3. Comparison of outlet apple juice concentration for five cases of RO networks

Scenario	Elements number	The decision variables $Q_{f(plant)}$(m³/s)	$P_{f(in)(plant)}$(kpa)	$T_{(in)(plant)}$(°C)	$°Brix_{out(plant)}$
A	1	5.00E-5	4200	49.22	14.84
	3	5.00E-5	4200	50.00	22.41
B	1	2.50E-5	4200	42.80	15.39
	3	2.50E-5	4200	44.66	23.67
C	1	2.50E-5	4200	42.51	15.40
	3	2.50E-5	4200	45.00	23.68
D	1	2.50E-5	4200	46.92	16.76
	3	3.68E-5	4200	45.00	**25.44**
E	1	1.00E-4	4200	35.50	12.08
	3	1.00E-4	4200	46.84	15.21

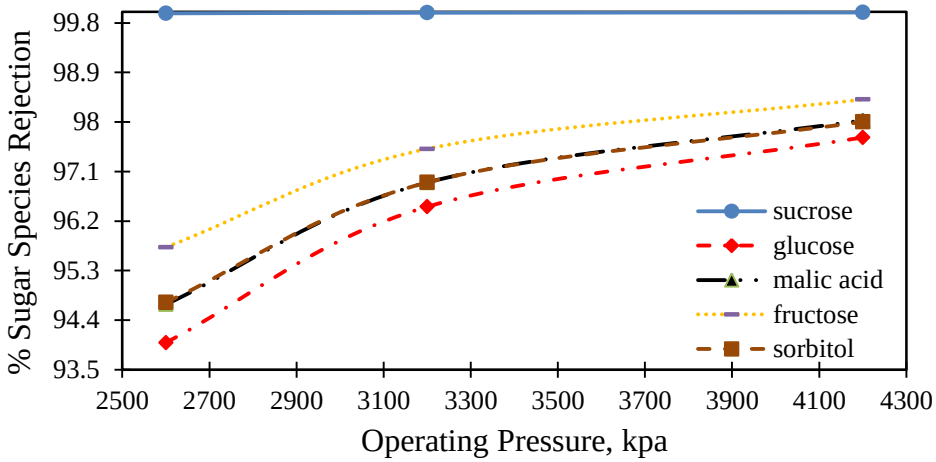

851

852 **Fig. 2**. Sugar species rejection as a function of operating pressure at inlet feed flow rate
853 and temperature of 1E-3 m³/s and 40 ℃
854

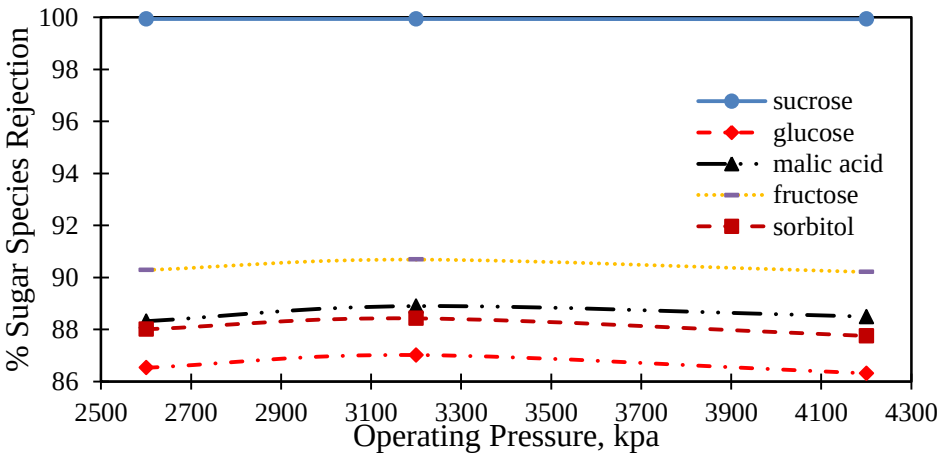

855

856 **Fig. 3**. Sugar species rejection as function of operating pressure at inlet feed flow rate
857 and temperature of 1E-4 m³/s and 40 ℃
858

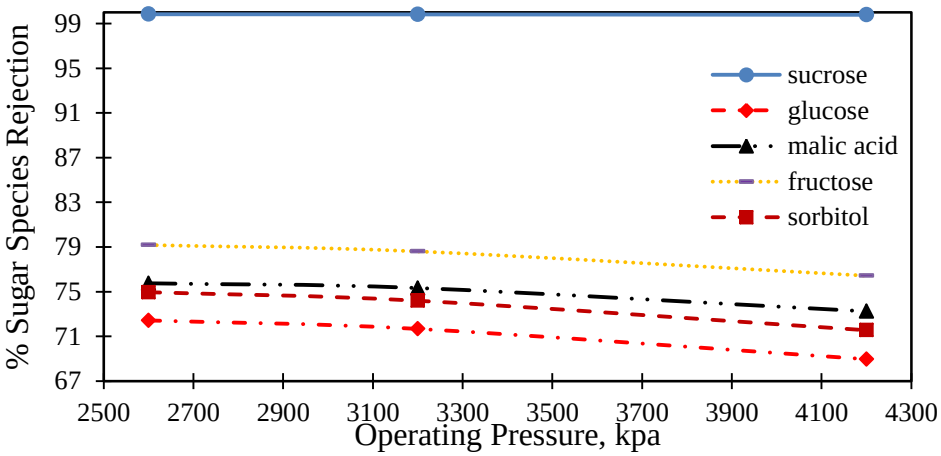

859

860 **Fig. 4**. Sugar species rejection as a function of operating pressure at inlet feed flow rate
861 and temperature of 3.7E-5 m³/s and 40 ℃

862

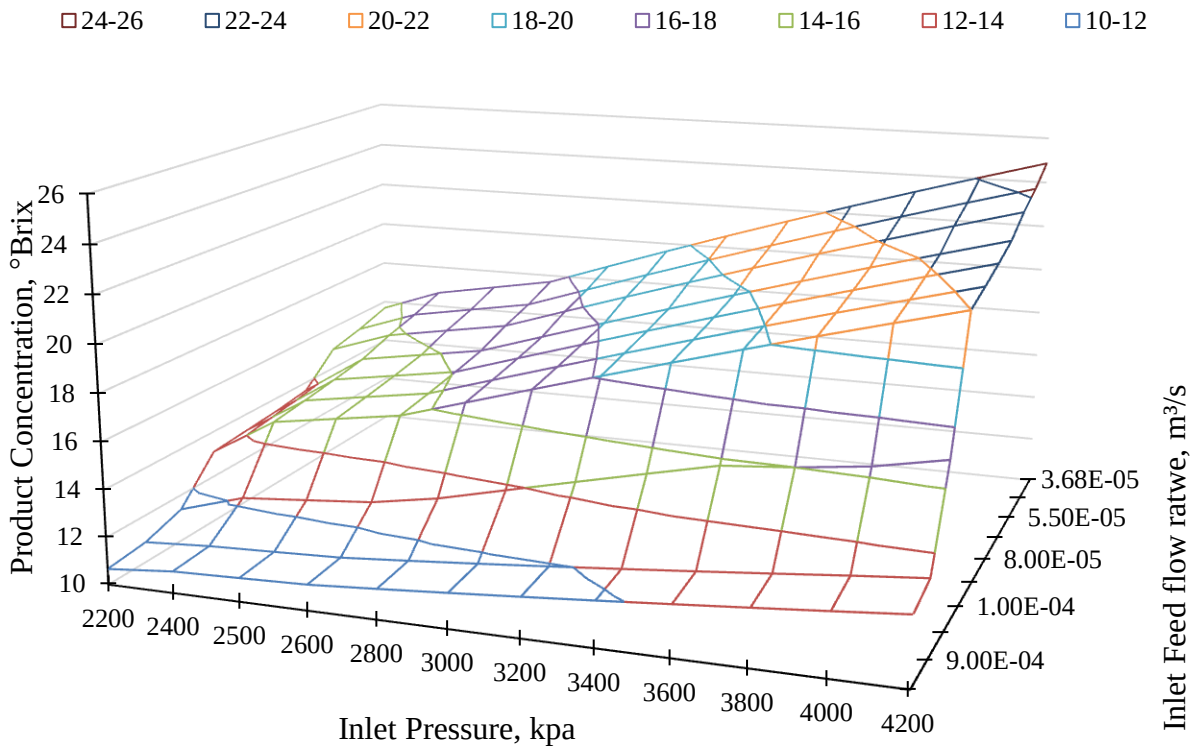

863

864 **Fig. 5**. Impact of variation in inlet feed pressure and flow rate on product concentration at fixed inlet feed
865 concentration and temperature of 10.5 °Brix and 40 °C

866

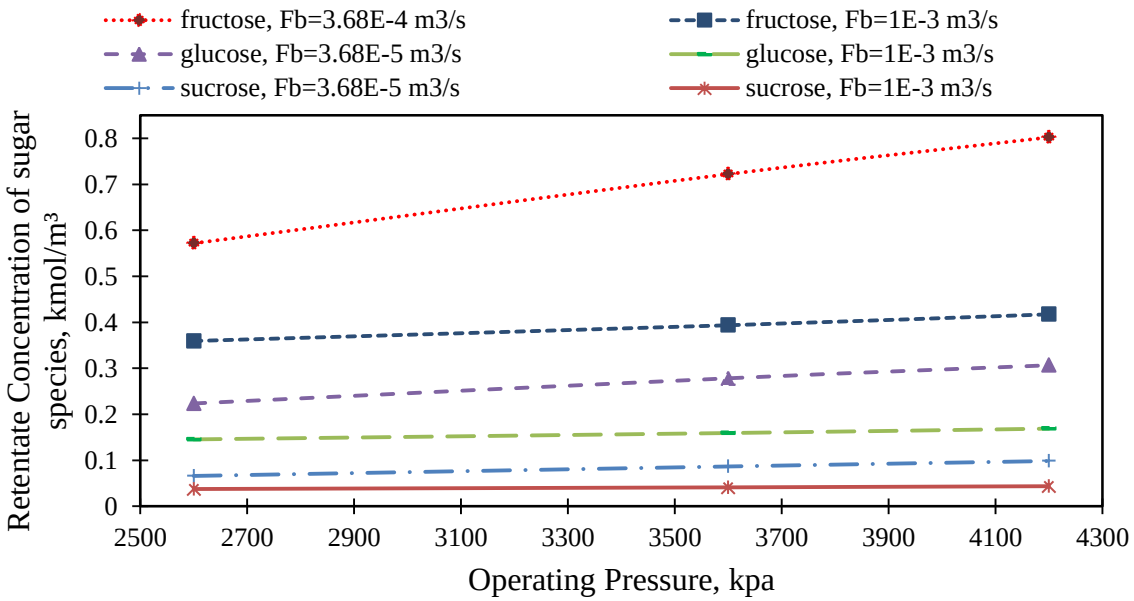

867

868 **Fig. 6**. Sugar species retention concentration verse operating pressure at two inlet feed flow rates and inlet feed
869 concentration and temperature of 3.68E-5 and 1E-3 m³/s, 10.5 °Brix and 40 °C

870

871

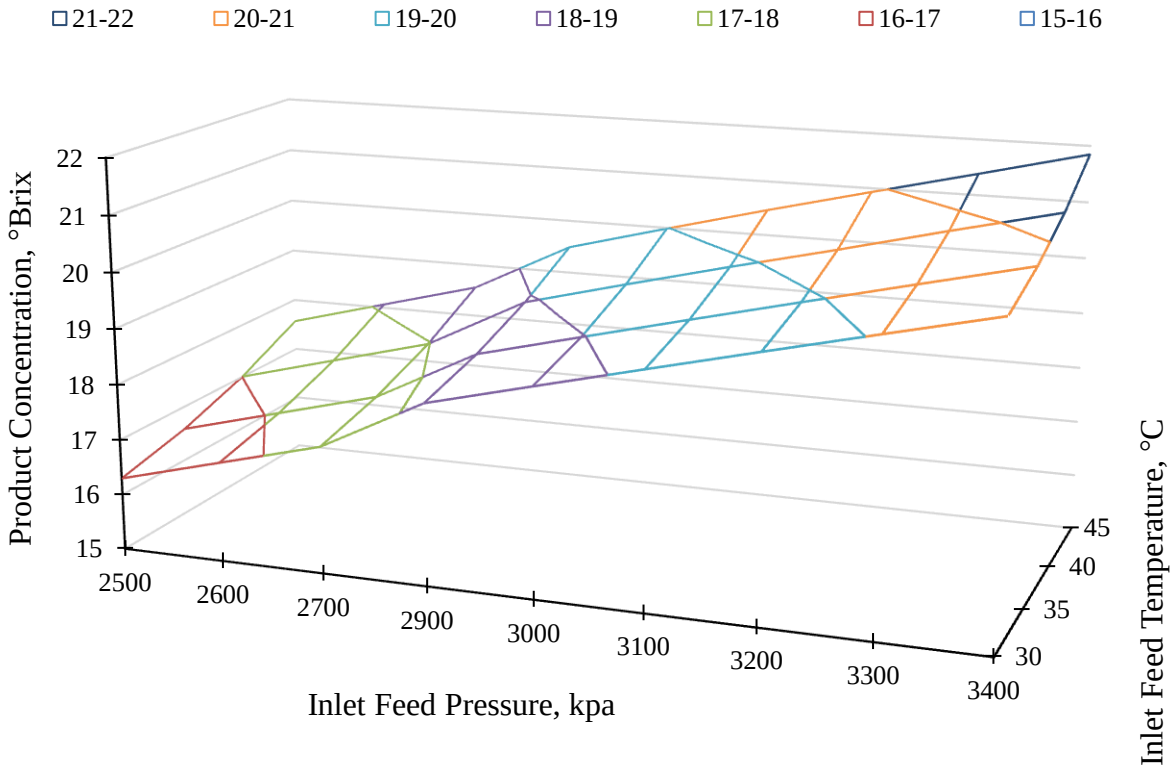

872

873 **Fig. 7**. Impact of variation in inlet feed pressure and temperature on product concentration at fixed inlet feed
874 concentration and flow rate of 10.5 °Brix and 4E-5 m³/s

875

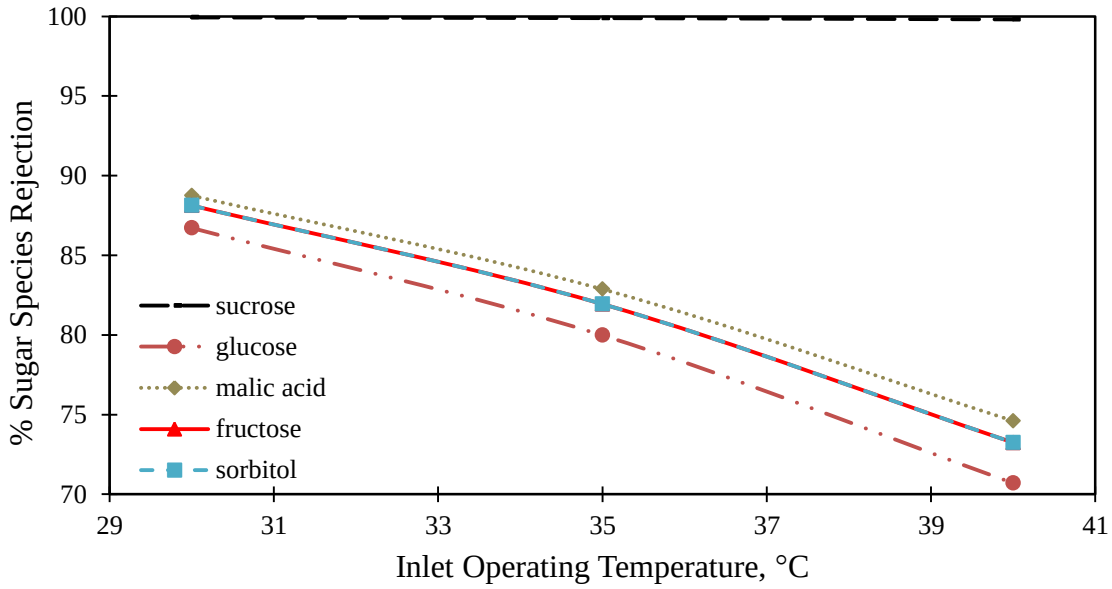

876

877 **Fig. 8**. Sugar species rejection as a function to operating feed temperature at inlet feed
878 concentration and flow rate of 10.5 Brix and 3.68E-5

879

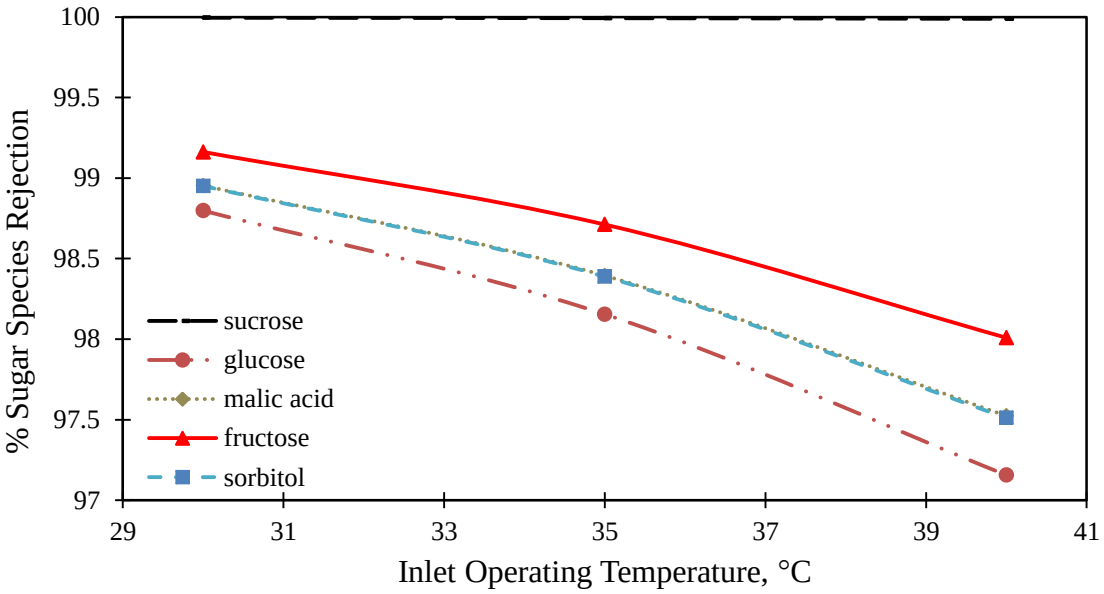

Fig. 9. Sugar species rejection as a function to operating feed temperature at inlet feed concentration and flow rate of 10.5 Brix and 1E-3